



CELLULAR AND MOLECULAR BIOLOGY

Correlation of *cGAS*, *STING*, *INF- α* and *INF- β* gene expression with Zika virus kinetics in primary culture of microglia and neurons from BALB/c mice

MAYQUE PAULO M. DE SOUZA, BÁRBARA CAROLINE G. FREITAS, GUSTAVO M. HOLANDA, JOSÉ ANTÔNIO P. DINIZ JUNIOR & ANA CECÍLIA R. CRUZ

Abstract: Pattern recognition receptors participate in the innate immune response. Among PRRs, the *cGAS*/*STING* pathway is known to detect cytosolic DNA and cyclic dinucleotides, but it's also important in RNA virus infection. We aimed to evaluate the gene expression of some important genes of *cGAS*/*STING* pathway and to correlate this expression with Zika virus kinetics in mice microglia and neurons. Cells were infected by MOI = 1.0. Indirect immunofluorescence, plaque titration of supernatant, extraction, and quantification of total intracellular RNA, RT-qPCR and Western blotting were performed. Plaque titration profile in microglia and neurons was similar, including higher titers of plaque forming units at 24, 48, 72 and 96 hpi, respectively. ZIKV kinetics evaluated by RT-qPCR was similar in both cells, with highest viral titers at 48, 72, 24 and 96 hpi, respectively. Expression profile of *cGAS*, *STING*, *INF- α* and *INF- β* was quite different between the cells, including gene suppression, as observed for *cGAS* in neurons. Our results showed a differentiated expression profile of *cGAS*/*STING* pathway genes in mice microglia and neurons, which can be explained by the different mechanisms that ZIKV uses to bypass the immune response of these cells. Furthermore, each cell type responds differently to combat the viral infection.

Key words: *cGAS*/*STING* pathway, *INF- α* , *INF- β* , primary cell cultures of CNS, viral kinetics, Zika virus.

INTRODUCTION

Grouped in the *Flaviviridae* family and belonging to the *Flavivirus* genus, the Zika Virus (ZIKV) is an enveloped arbovirus, that was firstly discovered and isolated in 1947, in Uganda, Africa (Dick et al. 1952). The ZIKV genome is composed by a single-stranded positive-sense ribonucleic acid (RNA), and the viral genetic material comprises a single Open Reading Frame (ORF), that after processing, generate ten mature proteins (Faye et al. 2014, Petersen et al. 2016).

In vertebrates, the innate immune system acts on the recognition of pathogen-associated

molecular patterns (PAMPs), derived from invading microorganisms, as well as damage-associated molecular patterns (DAMPs), derived from damages to the cell itself, as from the pattern recognition receptors (PRRs) (Kumar et al. 2011). Once activated, the PRRs commonly trigger a signaling cascade, which results in the induction of the expression of type I interferons (*INF-I*), inflammatory cytokines and chemokines (Hayashi et al. 2011) According to the literature, at least three classes of PRRs are related to the detection of flavivirus: toll-like receptors (TLR 3 and 7), capable of detecting viral RNA within the

endosome; receptors similar to the retinoic acid-inducible gene I (RIG-I), capable of detecting RNA species located in the cytoplasm; and cGAS/STING pathway, which detects cytoplasmic double stranded deoxyribonucleic acid (dsDNA) from damages caused by the flavivirus infection (Serman & Gack 2019, Ran et al. 2014).

The cGAS/STING pathway is a signaling pathway that has an active role in the detection of exogenous DNA, hybrids of DNA/RNA and cyclic dinucleotides (Nazmi et al. 2012, Li et al. 2013, Cai et al. 2014). However, many studies have been demonstrating that the cGAS/STING pathway is also an important agent in the detection of some RNA viruses, especially retrovirus, as HIV, for example (Lahaye et al. 2013, Vermeire et al. 2016). Dengue virus (DENV), Japanese encephalitis virus (JEV), West Nile virus (WNV), Zika virus (ZIKV), and severe acute respiratory syndrome-associated coronavirus (SARS-CoV), have been reported as antagonists of the cGAS/STING pathway (Aguirre et al. 2012, Maringer & Fernandez-Sesma 2014, Ding et al. 2018).

In humans, ZIKV is an antagonist of the cGAS/STING pathway and other important pathways related to the synthesis of type I interferon (INF-I). Nonetheless, in other mammals, such as immunocompetent mice, the virus is efficiently fought. (Grant et al. 2016, Conde et al. 2016, Eaglesham & Kranzusch 2020). The mechanisms used by ZIKV, as the cleavage of STING and STAT2 to evade the immune response in humans, but not in wide mice, contribute to the most effective primary immune response observed in murine models, in compare to the primary immune response in humans, since the virus successfully interrupts important pathways involved in INF-I synthesis and proinflammatory cytokines (Ding et al. 2018).

Once the use of adult immunocompetent mice would be a big challenge for experimental

ZIKV infection, because of the viral replication is interrupted by the innate immune response before the systemic spread of the virus (Aliota et al. 2016, Lazear et al. 2016), this study focused in the use of immunocompetent newborn mice and mice embryos, in order to obtain primary cultures susceptible and permissible to the ZIKV experimental infection, since newborn have not yet matured their immune systems to efficiently combat the viral infection (Li et al. 2016, Lum et al. 2017) and the ZIKV has great affinity for neural progenitor cells (NPCs) of the embryos (Souza et al. 2016). Therefore, the aim of this study was to evaluate the gene expression of genes involved in the cGAS/STING pathway, correlating with the ZIKV kinetics in primary cultures of BALB/c mice microglia and neurons, to thereby, determine the gene expression profile of those target genes, over the hours post infection.

MATERIALS AND METHODS

Mice

The present study was approved by the Committee for Ethics in Research on the use of Animals of the Evandro Chagas Institute (IEC; protocol No. 38/2018/CEUA/IEC/SVS/MS). A total of sixty pregnant albino mice of BALB/c lineage at 16 days of gestation and their one-day-old neonates from the colony of the Evandro Chagas Institute Central Animal House were used. All animals were maintained in standard plastic cages (32×39×16 cm) with water and food *ad libitum* under controlled temperatures (23±2°C) and a 12-h light/dark cycle.

Viral strain

All experimental assays were done using Zika virus (BE H 818308) confirmed by RT-qPCR from a case of human death in the Maranhão State, Brazil, provided by the IEC Arbovirology and Hemorrhagic Fever Department.

Primary culture of neurons

For primary cell culture of neurons, the whole brains were extracted from BALB/c mice embryos at embryonic day 16 (E16) after decapitation. In aseptically conditions to avoid contamination, the meninges and blood vessels were extracted in cold Hanks' balanced salt solution (HBSS) and the cells of the brain tissue were mechanically dissociated in HBSS. After decanting the non-dissociated tissue, the supernatant was transferred to 15.0 ml tubes, centrifuged at 300 G, for 5 minutes at 10°C, and the cell precipitate was resuspended in Neurobasal medium (Invitrogen/USA) supplemented with Glutamax (Thermo Fisher Scientific/USA), glutamate (25 µM) and B27 supplement (Thermo Fisher Scientific/USA). The cells were counted and seeded at 2.0×10^5 cells/well in 6-well plates previously treated with poly-L-lysine (Sigma Aldrich/USA) at a concentration of 12.5 µg / ml and incubated at 37°C under a humid atmosphere of 95% and 5% CO₂.

Primary culture of glial cells and microglia

For primary cell culture of glia cells, the euthanizing asepsis was performed with 70% ethanol in newborn BALB/c mouse (1 day of life), the brain was dissected, meninges and vessels removed, and the cells of the brain tissue were mechanically dissociated in HBSS. After decantation of the non-dissociated tissue, the supernatant was transferred to 15.0 ml tubes, centrifuged and the cell pellet was resuspended in glial medium [Dulbecco's Modified Eagle Medium (D-MEM/F12) (Thermo Fisher Scientific/USA)] containing 10% of fetal bovine serum (FBS). The cells were seeded at culture bottles of 75cm², previously treated with poly-L-lysine at a concentration of 12.5 µg/ml (Sigma Aldrich/USA). The cells were incubated at 37°C under a humid atmosphere of 95% and 5% CO₂.

Microglial cells were obtained from the cell culture of glia cells with two weeks of culture, being morphologically identified as shiny cells located on the cell monolayer. The microglia were released by hand agitation for a few minutes. The supernatant was collected and centrifuged at 300 G, for 5 minutes at 10°C. The cells were resuspended and maintained in D-MEM/F12 medium and kept in an oven at 37°C, under a humid atmosphere composed of 95% atmospheric air and 5% CO₂.

Viral infection

For all experiments, mice microglia and neurons were seeded at the density of 2.0×10^5 cells/well and infected with multiplicity of infection (MOI) = 1.0 at 24h and 72h, respectively.

Indirect Immunofluorescence (IIF)

MOCK (non-infected cells) and infected microglia and neurons at 24 hpi by MOI = 1.0, were fixed in 4% paraformaldehyde for 30 minutes. Then, washed 3x with PBS, permeabilized with 1% Triton X-100 solution in PBS and then incubated in PBS-50mM ammonium chloride. Blocking of nonspecific sites for both cell types was done with a solution containing 50% rabbit serum, 10% horse serum and 8% protein concentrate from the Mouse on Mouse (MOM®) kit (Maravai Life Sciences Inc./USA) in Phosphate Buffered Saline (PBS), pH 8.0 for 1 hour, then primary antibody against ZIKV (polyclonal anti-Zika antibodies) (1:50) produced at Evandro Chagas Institute and obtained from mice (host animal used for the production of primary antibodies) was incubated overnight in a wet chamber. In the next day, the samples were washed 3x with PBS and incubated with secondary antibody Alexa Fluor 488 Goat-anti-Mouse-anti-ZIKV (Dilution 1:500, Catalog #A-10680, Life Technologies./USA) for neurons and Alexa Fluor 568 Goat-anti-Mouse-anti-ZIKV for microglia (Dilution 1:500,

Catalog #A-11004, Life Technologies./USA), and posteriorly incubated with the cell nucleus marker DAPI (4', 6'-diamino-2-phenyl-indole) (1:200, Catalog #D1306) (Invitrogen™/USA) for 20 minutes and with anti-Iba1 primary antibodies (in microglia) and phalloidin (in the actin filaments of neurons) (1:200) in 0.1 M PBS, pH 7.2-7.4 for 20 minutes. After that, the coverslips were washed with PBS and mounted on slides with Prolong Antifade (Invitrogen/USA), observed and photographed by Leica TCS SP8 confocal microscope (Leica Microsystems/Germany).

Plaque titration of microglia and neuron supernatant

The viral titer of the samples was determined by plaque assays (Dulbecco & Vogt 1953). Briefly, Vero cell monolayers in six-well plates were incubated with 100 µL serial (log 10) dilutions of the viral sample at 37°C for 1 h under gentle shaking every 15 min. After this, medium 199 (Sigma-Aldrich, USA) containing non-adsorbed virus was replaced with a semi-solid culture medium (3% carboxymethylcellulose in medium 199) supplemented with 2% fetal bovine serum, 100 U/ml penicillin, and 100 µg/ml streptomycin. After 7 days at 37°C, the cells were fixed and stained with 0.1% cresyl violet solution, 30% ethanol, and 20% formaldehyde in PBS, and the cell death zones (plaques) were counted. The viral titer was calculated by multiplying the number of plaques obtained from a given viral serial dilution and, subsequently, by the dilution factor, with the result being reported in plaque-forming units per milliliter (PFU/ml).

RNA extraction

Automated RNA extraction from the MOCK and infected neurons and microglia was performed with the samples collected at 24, 48, 72 and 96 hpi, using Maxwell® 16 Total RNA Purification Cell Culture kit (Promega/USA). At the end

of extraction, the material was collected in a new microtube containing 50µL of RNase-free water and centrifuged for two minutes at 1.200 G, posteriorly the material was quantified by the Qubit 2.0 equipment, using the Qubit™ RNA HS Assay Kit (Thermo Fisher Scientific/USA) according to the manufacturer's protocol recommendations. In the end, the RNA extracted and quantified from all samples, was standardized to a final concentration of 50ng/µL and stored at -80 °C.

Viral RNA Quantification

The quantification of viral RNA was based on a standard curve with concentrations determined by serial dilution using a probe and primers described by Lanciotti et al. 2008, which bind to the region of the viral envelope, with a concentration of 200 and 300 nM, respectively. Quantification was performed by TaqMan probe methodology on the Rotor-Gene® Q equipment (Qiagen/Germany), using the Superscript® III Platinum® One Step RT-qPCR System kit (Invitrogen/USA), according to the manufacturer's protocol.

Gene Expression

RT-qPCR reactions to the target genes were performed with the GoTaq® 1-Step RT-qPCR System kit (Promega/USA) on the Rotor-Gene® Q equipment (Qiagen/Germany), according to the manufacturer's protocol, using the SYBR Green methodology. The cellular normalizing gene β -actin was used as an endogenous control. The primers pairs used to amplified the target genes (*cGAS*, *STING*, *INF- α* e *INF- β*) are listed in table I. The analysis of the mRNA quantification was performed by the $2^{-\Delta\Delta Ct}$ method using the Rotor-Gene® Q equipment (Qiagen/Germany), according to the manufacturer's instructions.

Table I. Primer pairs used to amplify the target genes.

Gene	Primer Forward (5' → 3')	Primer Reverse (5' → 3')
<i>STING</i>	CATTGGGTACTIONTTCGGTT	CTGAGCATGTTGTTATGTAGC
cGAS	ACGAGAGCCGTTTTATCTCGTACCC	TGTCCGGAAGATTCACAGCATGTTT
INF- α	ATAACCTCAGGGAACAAGA	GAGGAAGAGCAGGGCTCTC
INF- β	CGAGCAGAGATCTTCAGGAAC	TCACTACCAGTCCCAGAGTC
β -actin	GCGGGAAATCGTGCGTGACATT	GATGGAGTTGAAGGTAGTTTCGTG

Western Blotting

For the Western blotting assay, 1.0 ml of lysate suspension cells infected at 96 hpi, and MOCK, were used. After the cell lysis, the samples were concentrated in Amicon® Ultra-15 Centrifugal Filter Unit filters (100KDa) (Merck Millipore/USA). The Bradford Assay (Thermo Fisher Scientific/USA) was performed to protein quantitation, and a standardization curve was made with known concentrations of BSA protein read in absorbance at the 595nm. For greater reliability of the results, the linear correlation coefficient used, corresponded to a value greater than 0.98. All samples were standardized to 30 $\mu\text{g}/\mu\text{L}$, which was the final concentration of protein/well applied.

The samples were heated to 95°C for 5 minutes, centrifuged for 1,300 G for 5 minutes at 25°C, applied in SDS-polyacrylamide gel (SDS-PAGE) 10% and Stacking/Upper gel and submitted to electrophoresis at 100 volts for approximately 2 hours, with a ladder. After electrophoresis, the gel proteins were transferred to a nitrocellulose membrane, by mounting the sandwich cassette (negative support, sponge, filter paper, gel, membrane, filter paper, sponge, and positive support) at 100 volts and approximately 400mA for 1 hour, in a refrigerated environment and under agitation.

After the transfer stage, the membrane was blocked by incubation for 1 hour under agitation,

with Molico skimmed milk (Nestlé/Switzerland), at a concentration of 10% diluted in TBS-t, then, the membrane was washed (2x) with TBS-t for 10 minutes and incubated with the primary antibody (Anti-TMEM173) Rabbit-anti-Mouse (1:500) in TBS-t at 0.1% of Molico skimmed milk, overnight under agitation at low temperature.

In the next day, washes (1x) with TBS-t for 10 minutes and (2x) with TBS for 10 minutes, was made and the membrane was incubated for 1 hour with the secondary antibody (Alexa Fluor 568nm Goat-anti-Rabbit) (1:5,000) in TBS-t, under agitation and protected from light. Posteriorly, the membrane was washed (3x) with TBS for 10 minutes and revealed in the Typhoon™ FLA 9000 equipment (GE Healthcare Bio-Sciences AB/Sweden), at Alexa Fluor 555nm filter.

Statistical analysis

Statistical analyzes, graphs and figures were performed through analysis of variance (ANOVA) and *t* test of the results, with quantification graphs generated by the PRISM 8.0 tool. The level of significance analyzed was considered significant for *p* values ≤ 0.05 . All results were presented as mean and standard deviation.

RESULTS

The susceptibility of mice microglia and neurons to the ZIKV was confirmed by the indirect

immunofluorescence assay at 24 hpi (figure 1 and figure 2).

By the plate titration of the supernatant of microglia and neurons, the number of PFU/ml in neurons was higher than that microglia in all hour's post-infection verified, except at 24 hpi. Additionally, was observed that the number of plaques forming units (PFUs) decreased over the hours post-infection, with the highest numbers of PFUs observed at 24, 48, 72 and 96 hpi, respectively, for both cell types (table II).

The quantification analysis of viral RNA for MOI = 1.0 in microglia and neurons, showed varying concentrations over the hours post-infection, with viral titers being greater at 48, 72, 24 and 96 hpi, respectively, for both cell types.

In microglia, the expression levels of *cGAS*, *STING*, *INF- α* and *INF- β* genes was statistically

significant ($p < 0.05$), over the hours post-infection, in compared to the expression levels represented by the MOCK. In addition, the expression levels of the target genes over the hours post-infection were also statistically significant among the infected groups.

The highest levels of expression of the *cGAS*, *INF- α* and *INF- β* genes in microglia were observed at 48 hpi, on the other hand, the highest level of expression of the *STING* gene was observed at 72 hpi (figure 3). In microglia, the *STING* and *cGAS* genes had a higher expression rate than the MOCK (figure 3a, b), over the four analyzed periods, these expression rates being lower on 96 hpi for the *cGAS* gene and on 24 hpi for the *STING* gene. For the *INF- α* and *INF- β* genes, a reduction statistically significant in expression levels at 72 and 96 hpi was observed,

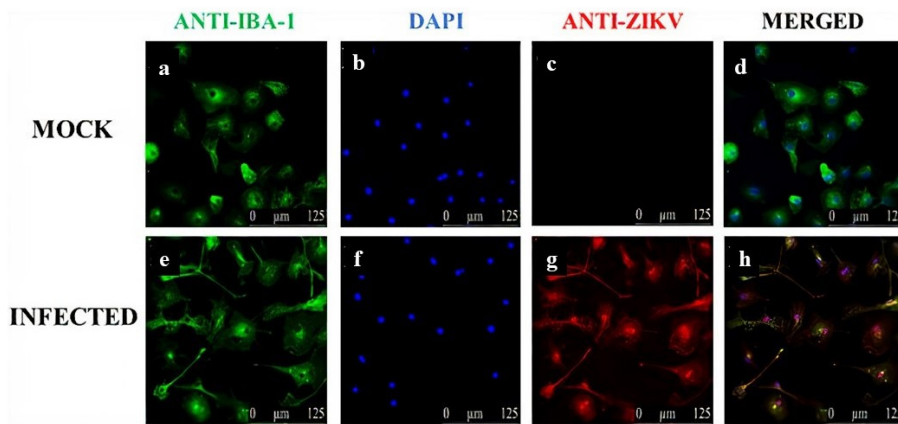


Figure 1. IIF of microglia cells at 24 hpi. **a)** Marking of iba-1 in microglia. **b)** Labeling of nucleic acids by DAPI. **c)** Absence of marking for ZIKV. **d)** Merged A, B and C images. **e)** Marking of iba-1 in microglia. **f)** Labeling of nucleic acids by DAPI. **g)** Presence of marking for ZIKV. **h)** Merged E, F and G images. Scale bar 125 μm . Microglia were seeded at 2.0×10^5 cells/well.

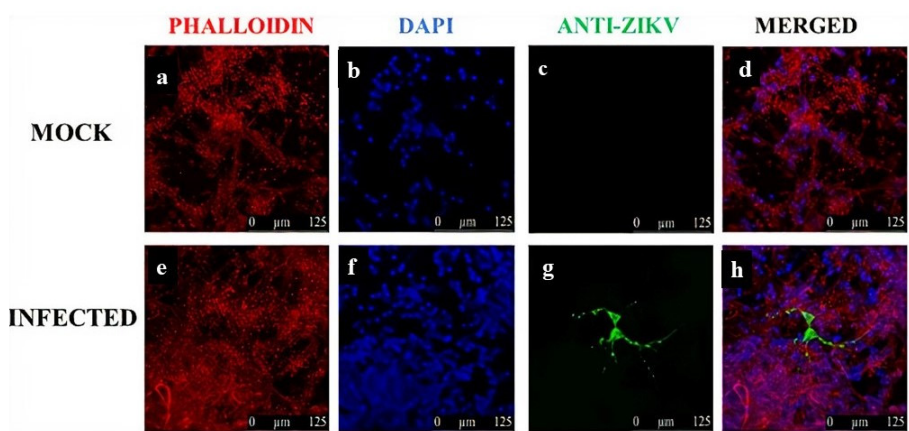


Figure 2. IIF of neurons cells at 24 hpi. **a)** Marking of actin filaments by phalloidin in neurons. **b)** Labeling of nucleic acids by DAPI. **c)** Absence of marking for ZIKV. **d)** Merged A, B and C images. **e)** Marking of actin filaments by phalloidin in neurons. **f)** Labeling of nucleic acids by DAPI. **g)** Presence of marking for ZIKV. **h)** Merged E, F and G images. Scale bar 125 μm . Neurons were seeded at 2.0×10^5 cells/well.

respectively (figure 3c, d). During the other periods analyzed, as well as in the *cGAS* and *STING* genes, an increase in the expression rates of these genes was observed, in comparison to MOCK (table III).

Regarding neurons, was observed that the gene expression of the four target genes was statistically significant ($p < 0.05$), in compared to the MOCK. In addition, the gene expression detected were also statistically significant among the infected groups over the hours post-infection for all the genes, except for the *cGAS* gene ($p = 0.4978$) (table IV).

The highest level of expression of *cGAS*, *STING* and *INF- β* genes in neurons were observed at 96 hpi, on the other hand, for the *INF- α* gene the period of greatest expression was observed it 72 hpi (figure 4). In comparison to the MOCK, the *cGAS* gene had a significant reduction in the level expression over the first three hours post-infection verified (there was also observed suppression of *cGAS* gene at 96 hpi, however this suppression was not statistically significant) (figure 4a).

About *STING* gene, at 24 and 48 hpi was detected increased gene expression in compared to the MOCK, however, these reductions were not statistically significant. On the other hand, there was a statistically significant increase of *STING* expression at 72 and 96 hpi in the infected group (figure 4b).

The *INF- α* gene had increased expression at 96 hpi, which was also observed to be the only hour post-infection on which there was a statistically significant reduction in the gene expression in compared to the MOCK. On the other hand, at 24, 48 and 72 hpi the levels of *INF- α* gene were higher than the MOCK, which 72 hpi showing the highest expression rate, and the unique period of statistically significant increase (figure 4c).

Table II. Plaque titration of supernatant of BALB/c mice microglia and neurons for each hour post-infection. A higher number of PFU/ml was observed at 24, 48, 72 and 96 hpi, respectively, for both cell types. Both cells were seeded at 2.0×10^5 cells/well.

Hour post infection (hpi)	Microglia	Neuron
24h	$2,45 \times 10^4$ PFU/ml	$2,00 \times 10^4$ PFU/ml
48h	$1,30 \times 10^3$ PFU /ml	$5,00 \times 10^3$ PFU/ml
72h	$1,00 \times 10^3$ PFU/ml	$1,30 \times 10^3$ PFU/ml
96h	$5,00 \times 10^2$ PFU/ml	$7,00 \times 10^2$ PFU/ml

Compared to MOCK, the lowest level of *INF- β* expression was observed at 24 hpi, it was also the only hour post-infection that showed reduction of expression for this gene, being this reduction statistically significant. On the other hand, was observed that *INF- β* expression was higher and statistically significant than the MOCK at 48, 72 and 96 hpi, with 96 hpi being the period of greatest gene expression (figure 4d).

In the Western blotting assay, was detected bands in the expected molecular weight of the whole protein (~42 kDa) in both infected cells and in the MOCK, suggesting that *STING* protein from mice microglia and neurons was not cleaved (figure 5).

DISCUSSION

Generally, mice are widely used as experimental models, because of their numerous benefits that includes relatively low cost, ease of accommodation and handling. About studies involving ZIKV, mostly of them are conducted in mice with genetic deficiencies or acquired in interferon signaling, since the ZIKV is unable to efficiently antagonize the STAT2 protein of adult mice, which make immunocompetent mice resistant to the infection (Lazear et al. 2016, Morrison & Diamond 2017).

The primary culture of microglia and neurons from BALB/c mice, showed susceptibility for the isolated ZIKV strain (figures 1 and 2). The results of ZIKV kinetics in those cells, suggested a higher permissiveness of neurons to the isolated ZIKV, once the viral replication in neuronal cells was greater than microglia, over the four periods investigated. Our results were similar to the findings described by Costa et al. 2017, which infected ZIKV in primary cultures of neurons and glial cells of C57BL/6 mice and verified higher levels of viral titers at 48 and 72 hpi. The authors also observed greater permissiveness of ZIKV in

neurons in compared to glial cells, what caused massive neuronal damage in the primary culture of neurons, which may be related to the Congenital Syndrome Associated with Zika Virus Infection, reported in many newborns around the world (Chimelli et al. 2017, Desai et al. 2017).

Using MOI = 0.1 in human astrocytes and microglia, Ojha et al. 2019, compared the experimental *in vitro* infection of three isolated ZIKV strains, MR766 (Uganda), R103451 (Honduras) and PRVABC59 (Puerto Rico), and observed that in astrocytes, the viral titers of the three strains, were higher at 48 hpi and 72 hpi, respectively,

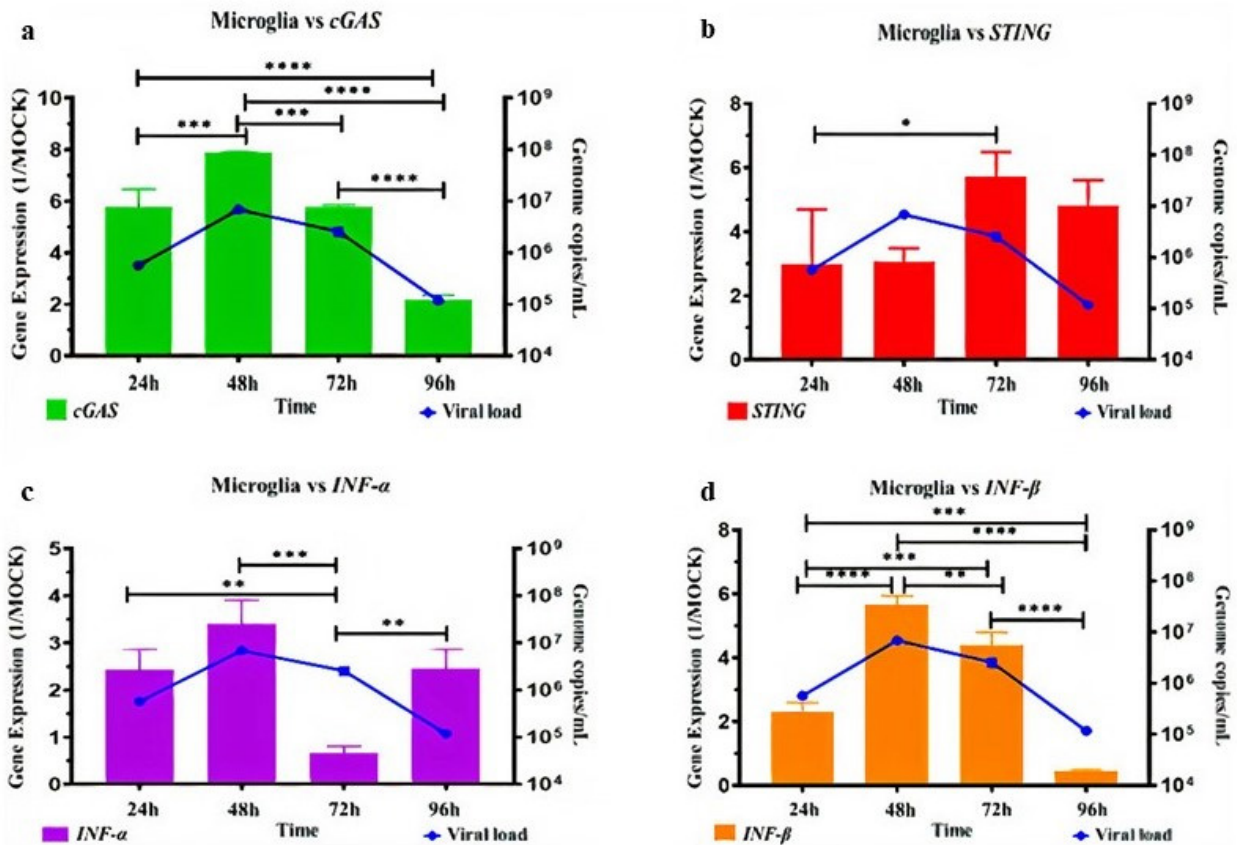


Figure 3. Correlation between the gene expression determined by RT-qPCR of *cGAS*, *STING*, *INF-α* and *INF-β*, in mice microglia experimentally infected with ZIKV, and the ZIKV kinetics in this cell type. The values of each hpi represent the average of results in triplicate. a) The *cGAS* expression was statistically significant increase at 24, 48, 72 and 96 hpi. b) *STING* expression was increased at 24, 48, 72 and 96 hpi, but only statistically significant at 24, 48 and 72 hpi. c) *Inf-α* expression was statistically significant increase at 24, 48, and 96 hpi, and statistically significant decrease at 72 hpi. d) The *Inf-β* expression was statistically significant decrease at 96 dpi, and increased at 24, 48 and 72 hpi, being the 48 hpi the unique period of statistically significant increase. Microglia were seeded at 2.0×10^5 cells/well and the MOI = 1.0. One-way ANOVA (Graph Prism 8.0) was the statistical test used.

and the R103451 strain, presented higher titles at 48, 72, 24 and 96 hpi, respectively, which was the same kinetics profile noticed for our isolated ZIKV strain. Similar results also were related by Souza et al. 2016, which determined the ZIKV kinetics by RT-qPCR at MOI = 0.1 in Induced Pluripotent Stem Cells (iPSCs), derived from humans.

The differences between the results observed in the plate titration experiment using the supernatant, and the ZIKV kinetics using the intracellular content, can be justified due the number of virions being lower in the supernatant, compared to the amount of viral genetic material in the intracellular environment, which is also the location where the virus replicates. It is also important to emphasize that the viral kinetics determined by RT-qPCR detects the genetic material, which is in greater quantity

when compared to the number of mature viral particles, what are used to determine the viral title in the plate titration test. Additionally, as results of cell death over the days because of the infection, fewer cells will be available for new infections, so, the amount of mature viral particles tends to decrease, how it was noted in our study.

The cGAS/STING pathway can detect and restrict flavivirus infection, such as DENV infection, which due to the damages in the mitochondrial membrane, the mitochondrial DNA (mtDNA) is exposed to the cytoplasm, thus leading to the recognition by cGAS protein and, consequently, the induction of INF-I (Aguirre et al. 2012, Schoggins et al. 2014). Most of the PAMPs and DAMPs recognized by PRRs during the ZIKV infection are still unknown, however, in humans, is known that the ZIKV infection also induces the

Table III. p values obtained by one-way ANOVA (Graph Prism 8.0), for cGAS, STING, INF- α and INF- β genes, in BALB/c microglia experimentally infected with ZIKV. The table below shows whether there was statistical significance of the infected groups when compared to the MOCK (t test), as well as whether there were statistical differences between the infected groups.

Gene	Hour post infection (hpi)	Fold change infected cells/NC	Statistical significance of each hpi in relation to the MOCK	p values (one-way ANOVA) compared to the MOCK	p values (one-way ANOVA) among the infected groups
cGAS	24h	5,7629	*	<0,0001	<0,0001
	48h	7,9007	***		
	72h	5,7821	**		
	96h	2,1798	**		
STING	24h	2,9779	***	0,0010	0,0314
	48h	3,0777	***		
	72h	5,7188	**		
	96h	4,8145	n.s		
INF- α	24h	2,4259	****	<0,0001	0,0002
	48h	3,4032	**		
	72h	0,6664	**		
	96h	2,4549	***		
INF- β	24h	2,3123	n.s	<0,0001	<0,0001
	48h	5,6544	**		
	72h	4,3852	n.s		
	96h	0,4586	***		

NC = Normalized Control (n.s = not significant $p > 0.05$; * $p < 0.05$; ** $p < 0.01$; *** $p < 0.001$; **** $p < 0.0001$ One-way ANOVA).

release of mtDNA into the cytoplasm, which is identified as a ligand for cGAS. Still not possible to say for sure if the cGAS protein detects only mtDNA during ZIKV infection, or if others host DNA species are detected (Zheng et al. 2018). Additionally, ZIKV utilizes an indirect strategy to evade the cGAS/STING response by the NS1 protein that stabilizes caspase-1 leading to the cGAS protein cleavage (Eaglesham & Kranzusch 2020).

Studies using knockout mice or cells derived from them, have been shown that mice without one or more components of the IFN-I system are susceptible to several ZIKV strains with high viral loads detected in the central nervous systems (CNS) and testicles, thus suggesting that the components of the IFN-I system, which

include PRRs, are in fact important members in the combat against the viral infection, since immunocompetent mice are able to efficiently stop viral infection caused by ZIKV (Ding et al. 2018, Lazear et al. 2016, Rossi et al. 2016). Interestingly, Azamor et al. 2021, demonstrated that Congenital Zika Syndrome (CZS) is associated with exacerbated IFN-I synthesis, and other study conducted by Silva-Filho et al. 2021, showed that infection of C57BL/6 mouse with ZIKV pre-treated with recombinant Gas6 (growth arrest-specific 6 protein) (ZIKV Gas6) facilitates ZIKV infection and leads to malformations in the offspring, which also is associated with upregulation of INF- α and INF- β .

Part of the divergent observations between human and mice, can be justified by the fact

Table IV. *p* values obtained by one-way ANOVA (Graph Prism 8.0), for *cGAS*, *STING*, *INF- α* and *INF- β* genes, in BALB/c neurons experimentally infected with ZIKV. The table below shows whether there was statistical significance of the infected groups when compared to the MOCK (t test), as well as whether there were statistical differences between the infected groups.

Gene	Hour post infection (hpi)	Fold change infected cells/NC	Statistical significance of each hpi in relation to the MOCK	<i>p</i> values (one-way ANOVA) compared to the MOCK	<i>p</i> values (one-way ANOVA) among the infected groups
<i>cGAS</i>	24h	0,2253	****	0,0082	0,4978
	48h	0,1635	***		
	72h	0,3815	*		
	96h	0,4592	n.s		
<i>STING</i>	24h	0,8462	n.s	<0,0001	<0,0001
	48h	0,5717	n.s		
	72h	3,7116	***		
	96h	22,3864	****		
<i>INF-α</i>	24h	1,0313	n.s	0,0002	0,0009
	48h	3,3625	n.s		
	72h	6,5328	****		
	96h	0,1444	****		
<i>INF-β</i>	24h	0,6466	*	<0,0001	<0,0001
	48h	6,1694	***		
	72h	6,3324	***		
	96h	8,1918	****		

NC = Normalized Control (n.s = not significant $p > 0.05$; * $p < 0.05$; ** $p < 0.01$; *** $p < 0.001$; **** $p < 0.0001$ One-way ANOVA).

that ZIKV uses several mechanisms to try to circumvent the human immune response, such as the inhibition of the C9 protein multimerization of the complement system and the deposition of the membrane attack complex in cells by the viral protein NS1 (Eaglesham & Kranzusch 2020) degradation of human STAT2, but not in mice (Kumar et al. 2016, Hai et al. 2019, Wang et al. 2020) as well as, the human STING protein be degraded, by the NS2B/3 ZIKV protease and by others flaviviruses related to ZIKV (Ding et al. 2018) The same, however, is not observed in immunocompetent mice, thus suggesting that

the cleavage of STAT2 and STING protein by ZIKV be a species-specific cleavage (Maringer & Fernandez-Sesma 2014).

The differences in the gene expression profiles in microglia and neurons may be related to the fact that, even though these cells make part of the same tissue, microglia are known to be CNS defense cells (Wake & Fields 2011), whereas neurons are cells responsible for conducting of nervous impulse and signal processing (Sardi et al. 2017), therefore, higher levels of gene expressions involved in the cell defense were expected in microglia, in compare

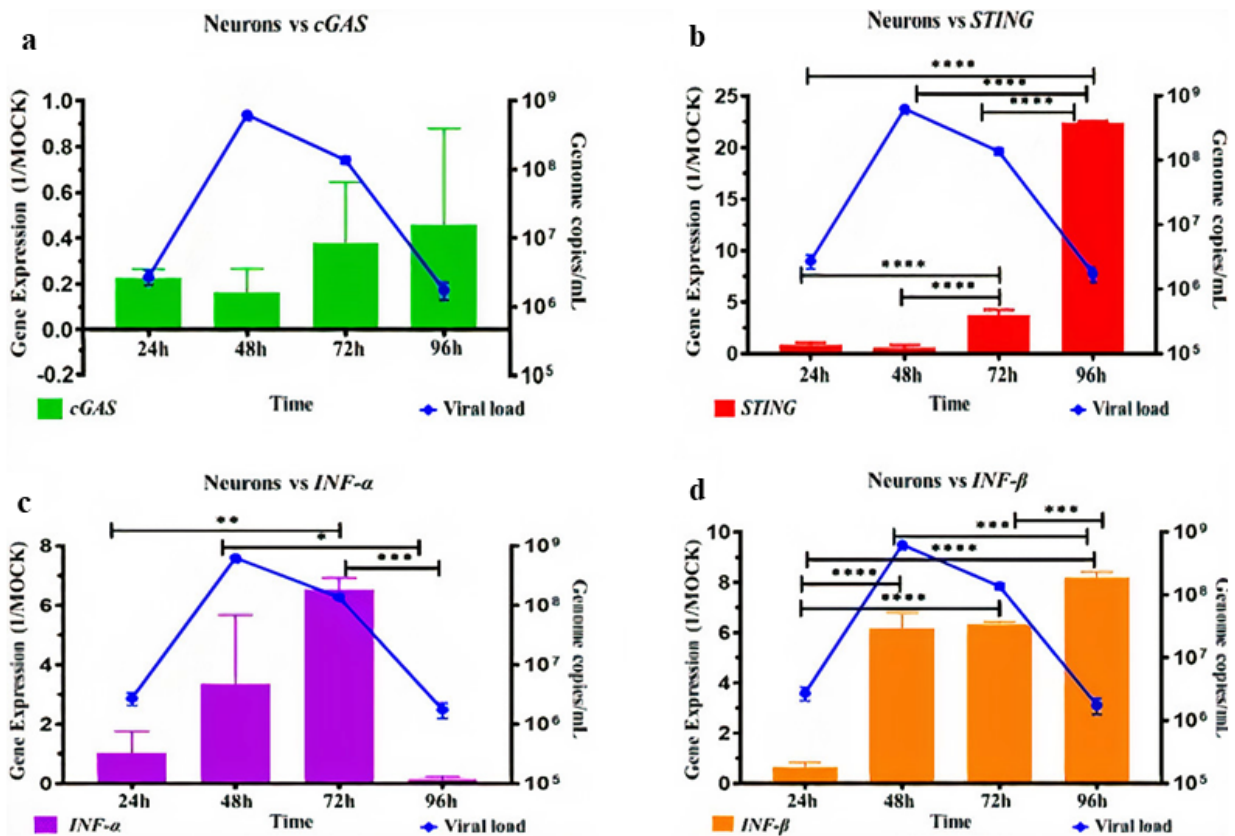


Figure 4. Correlation between the gene expression determined by RT-qPCR of *cGAS*, *STING*, *INF-α* and *INF-β*, in mice neurons experimentally infected with ZIKV, and the ZIKV kinetics in this cell type. The values of each hpi represent the average of results in triplicate. **a)** The *cGAS* expression was statistically decreased at 24, 48, 72 and decreased, but not statistically significant, at 96 hpi **b)** *STING* expression was decreased, but not statistically significant at 24 and 48 hpi, and statistically increased at 72 and 96 hpi. **c)** Expression of *INF-α* showed that there was a statistical decrease at 96 hpi, and increase at 24, 48 and 72 hpi, being statistically significant only at 72 hpi. **d)** Expression of *INF-β* showed that there was a statistical decrease at 24 hpi, and a statistical increase at 48, 72 and 96 hpi. Neurons were seeded at 2.0×10^5 cells/well and the MOI = 1.0. One-way ANOVA (Graph Prism 8.0) was the statistical test used.

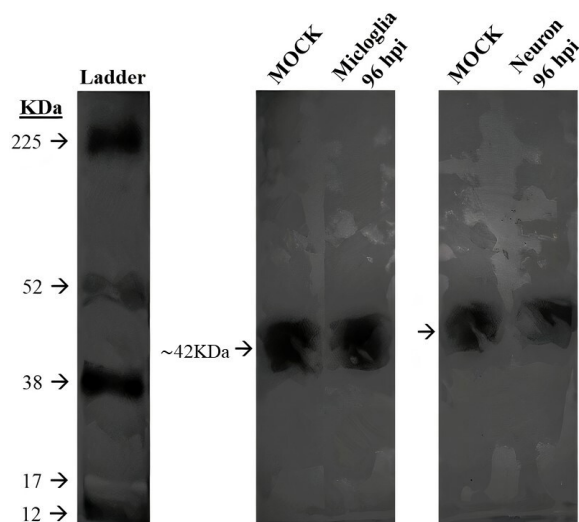


Figure 5. Western blotting assay for mice microglia and neurons STING protein. Bands were observed between the intervals of 52 and 38 kDa, in MOCK and in the infected cells at 96 hpi, suggesting that the murine STING (~42 kDa) was not cleaved by the ZIKV. For the western blotting assay microglia and neurons were seeded at 2.0×10^5 cells/well and the MOI = 1.0.

to neurons, as well as, higher levels in the periods with higher viral loads, once our work used cells from immunocompetent newborn mice and mice embryos.

The relationship between ZIKV viral load and the differences in the gene expression of the target genes, may be related to the different PRRs that act in the ZIKV detection (TLRs, RIG-I and cGAS/STING pathway), since these sensors probably operate together to identify possible combinations of PAMPs and DAMPs from ZIKV infection, or even, these PRRs act in a specific way for each cell type (Serman & Gack 2019, Vanwalscappel et al. 2018, Hu et al. 2019). Therefore, determining the contribution of each innate immunity sensors in different cell types and tissues, will be of great importance to better understand the course of ZIKV infection, as well as will help to contribute to the choice of which animal models and cell types that best fits for each type of intended study (Serman & Gack 2019).

In the Western blotting assay, for the infected group at 96 hpi, similar bands were observed in the MOCK, which refer to the expected molecular weight of murine STING protein (~42 kDa), suggesting that the cleavage of STING protein of microglia and neurons from BALB/c mice, did not happen. The same observation was reported by Ding et al. 2018, who showed that STING protein of fibroblasts from C57BL/6 mice and non-human primates (NHP) is not cleaved by the ZIKV, differently that was showed by the same authors with the human STING, which was cleaved by the viral protease (NS2B/3) between the 78/79 position. This cleavage restricted to humans, can be explained by the fact that the STING protein is only partially conserved in rodents and NHP.

In conclusion, our results showed a differentiated expression profile of cGAS, STING, *INF- α* and *INF- β* , in mouse microglia and neurons, even with similar viral load found for both cells in every day analyzed, thus suggesting that ZIKV may be using different mechanisms to bypass the immune response of each infected cell type. Additionally, it is known that different PRRs are involved in the detection of viral infection, as well as that each cell type, even if coming from the same species and tissue, responds differently to the viral infection, which may have contributed to the differences of gene expression found between microglia and neurons in this work.

Acknowledgments

We thank for the financial support Coordenação de Aperfeiçoamento de Pessoal de Nível Superior (CAPES) and Conselho Nacional de Desenvolvimento Científico e Tecnológico (CNPq). To Dr. Ana Paula Drummond Rodrigues for her help with the revelation of the western blotting membranes and Ana Flávia Oliveira de Oliveira for all her support with the primary cell culture.

REFERENCES

- AGUIRRE S ET AL. 2012. Denv inhibits type I IFN production in infected cells by cleaving human STING. *PLoS Pathogens* 8: 1-14.
- ALIOTA MT, CAINE EA, WALKER EC, LARKIN KE, CAMACHO E & OSORIO JE. 2016. Characterization of lethal Zika virus infection in ag129 mice. *PLoS Negl Trop Dis* 10: 1-11.
- AZAMOR T ET AL. 2021. Congenital Zika Syndrome is associated with interferon alfa receptor 1. *Front Immunol* 12: 764746.
- CAI X, CHIU Y-H & CHEN ZJ. 2014. The cGAS-cGAMP-sting pathway of cytosolic DNA sensing and signaling. *Molecular Cell* 54: 289-296.
- CHIMELLI L ET AL. 2017. The spectrum of neuropathological changes associated with congenital Zika virus infection. *Acta Neuropathol* 133: 983-999.
- CONDE JN, DA SILVA EM, ALLONSO D, COELHO DR, ANDRADE IS, DE MEDEIROS LN, MENEZES JL, BARBOSA AS & MOHANA-BORGES R. 2016. Inhibition of the membrane attack complex by Dengue virus NS1 through interaction with vitronectin and terminal complement proteins. *J Virol* 90: 9570-9581.
- COSTA VV ET AL. 2017. N-Methyl-D-Aspartate (Nmda) receptor blockade prevents neuronal death induced by Zika virus infection. *mBio* 8: e00350-17.
- DESAI SK, HARTMAN SD, JAYARAJAN S, LIU S & GALLICANO GI. 2017. Zika Virus (Zikv): a review of proposed mechanisms of transmission and associated congenital abnormalities. *Am J Stem Cells* 6: 13-22.
- DICK GWA, KITCHEN SF & HADDOW AJ. 1952. Zika Virus (I). Isolations and serological specificity. *Trans R Soc Trop Med Hyg* 46: 509-520.
- DING Q, GASKA JM, DOUAM F, WEI L, KIM D, BALEV M, HELLER B & PLOSS A. 2018. Species-specific disruption of STING-dependent antiviral cellular defenses by the Zika virus NS2B3 protease. *PNAS* 115: e6310-e6318.
- DULBECCO R & VOGT M. 1953. Some problems of animal virology as studied by the plaque technique. *Cold Spring Harb Symp Quant Biol* 18: 273-279.
- EAGLESHAM JB & KRANZUSCH PJ. 2020. Conserved strategies for pathogen evasion of cGAS-STING immunity. *Curr Opin Immunol* 66: 27-34.
- FAYE O, FREIRE CCM, IAMARINO A, FAYE O, DE OLIVEIRA JVC, DIALLO M, ZANOTTO PMA & SALL AA. 2014. Molecular evolution of Zika virus during its emergence in the 20th century. *PLoS Negl Trop Dis* 8: e2636.
- GRANT A ET AL. 2016. Zika virus targets human STAT2 to inhibit type I interferon signaling. *Cell Host & Microbe* 19: 882-890.
- HAI R, WANG B, THURMOND S & SONG J. 2019. Suppression of human STAT2 by Zikv NS5. *J Immunol* 202: 127-20.
- HAYASHI T, NAKAMURA T & TAKAOKA A. 2011. Pattern recognition receptors. *Nihon Rinsho Meneki Gakkai Kaishi* 34: 329-345.
- HUY ET AL. 2019. Zika virus antagonizes interferon response in patients and disrupts RIG-I-MAVS interaction through its CARD-TM domains. *Cell Biosci* 9: 1-15.
- KUMAR A, HOU S, AIRO AM, LIMONTA D, MANCINELLI V, BRANTON W, POWER C & HOBMAN TC. 2016. Zika virus inhibits type-I interferon production and downstream signaling. *EMBO* 17: 1766-1775.
- KUMAR H, KAWAI T & AKIRA S. 2011. Pathogen recognition by the innate immune system. *Int Rev Immunol* 30: 16-34.
- LAHAYE X, SATOH T, GENTILI M, CERBONI S, CONRAD C, HURBAIN I, EL MARJOU A, LACABARATZ C, LELIÈVRE J-D & MANEL N. 2013. The capsids of HIV-1 and HIV-2 determine immune detection of the viral cDNA by the innate sensor cGAS in dendritic cells. *Immunity* 39: 1132-1142.
- LANCIOTTI RS, KOSOY OL, LAVEN JJ, VELEZ JO, LAMBERT AJ, JOHNSON AJ, STANFIELD SM & DUFFY MR. 2008. Genetic and serologic properties of Zika virus associated with an epidemic, Yap State, Micronesia, 2007. *Emerg Infect Dis* 14: 1232-1239.
- LAZEAR HM, GOVERO J, SMITH AM, PLATT DJ, FERNANDEZ E, MINER JJ & DIAMOND MS. 2016. A mouse model of Zika virus pathogenesis. *Cell Host & Microbe* 19: 720-730.
- LI C, XU D, YE Q, HONG S, JIANG Y, LIU X, ZHANG N, SHI L, QIN C-F & XU Z. 2016. Zika virus disrupts neural progenitor development and leads to microcephaly in mice. *Cell Stem Cell* 19: 120-126.
- LI X-D, WU J, GAO D, WANG H, SUN L & CHEN ZJ. 2013. Pivotal roles of cGAS-cGAMP signaling in antiviral defense and immune adjuvant effects. *Science* 341: 1390-1394.
- LUM F-M, LOW DKS, FAN Y, TAN JYL, LEE B, CHAN JKY, RÉNIA L, GINHOUX F & NG LFP. 2017. Zika virus infects human fetal brain microglia and induces inflammation. *Clin Infect Dis* 64: 914-920.
- MARINGER K & FERNANDEZ-SESMA A. 2014. Message in a bottle: lessons learned from antagonism of STING signalling during RNA virus infection. *Cytokine & Growth Factor Rev* 25: 669-679.

MORRISON TE & DIAMOND MS. 2017. Animal models of Zika virus infection, pathogenesis, and immunity. *J Virol* 91: e00009-17.

NAZMI A, MUKHOPADHYAY R, DUTTA K & BASU A. 2012. Sting mediates neuronal innate immune response following Japanese encephalitis virus infection. *Sci Rep* 2: 347-357.

OJHA CR, RODRIGUEZ M, KARUPPAN MKM, LAPIERRE J, KASHANCHI F & EL-HAGE N. 2019. Toll-like receptor 3 regulates Zika virus infection and associated host inflammatory response in primary human astrocytes. *PLoS ONE* 14: e0208543.

PETERSEN LR, JAMIESON DJ, POWERS AM & HONEIN MA. 2016. Zika virus. *NEJM* 374: 1552-1563.

RAN Y, SHU H-B & WANG Y-Y. 2014. MITA/STING: A central and multifaceted mediator in innate immune response. *Cytokine & Growth Factor Rev* 25: 631-639.

ROSSI SL, TESH RB, AZAR SR, MURUATO AE, HANLEY KA, AUGUSTE AJ, LANGSJOEN RM, PAESSLER S, VASILAKIS N & WEAVER SC. 2016. Characterization of a novel murine model to study Zika virus. *Am J Trop Med Hyg* 94: 1362-1369.

SARDI S, VARDI R, SHEININ A, GOLDENTAL A & KANTER I. 2017. New types of experiments reveal that a neuron functions as multiple independent threshold units. *Sci Rep* 7: 18036.

SCHOGGINS JW ET AL. 2014. Pan-viral specificity of IFN-induced genes reveals new roles for cGAS in innate immunity. *Nature* 505: 691-695.

SERMAN TM & GACK MU. 2019. Evasion of innate and intrinsic antiviral pathways by the Zika virus. *Viruses* 11: 970-989.

SILVA-FILHO JL ET AL. 2021. Gas6 drives Zika virus-induced neurological complications in humans and congenital syndrome in immunocompetent mice. *Brain Behav Immun* 97: 260-274.

SOUZA BSF ET AL. 2016. Zika virus infection induces mitosis abnormalities and apoptotic cell death of human neural progenitor cells. *Sci Rep* 6: 39775.

VANWALSCAPPEL B, TADA T & LANDAU NR. 2018. Toll-like receptor agonist R848 blocks Zika virus replication by inducing the antiviral protein viperin. *Virology* 522: 199-208.

VERMEIRE J ET AL. 2016. HIV triggers a cGAS-dependent, VPU- and VPR-regulated type I interferon response in CD4+ T cells. *Cell Reports*. 17: 413-424.

WAKE H & FIELDS RD. 2011. Physiological function of microglia. *Neuron Glia Biol* 7: 1-3.

WANG B ET AL. 2020. Structural basis for STAT2 suppression by flavivirus NS5. *Nat Struct Mol Biol* 27: 875-885.

ZHENG Y, LIU Q, WU Y, MA L, ZHANG Z, LIU T, JIN S, SHE Y & CUI J. 2018. Zika virus elicits inflammation to evade antiviral response by cleaving cGAS via NS1-caspase-1 axis. *EMBO J* 37: e99347.

ABBREVIATIONS

ANOVA = Analysis of variance

BALB/c = Albino mice (*Mus musculus* BALB/c)

cGAMP = 2'3'-Cyclic GMP-AMP

cGAS = Cyclic GMP-AMP synthase
CMC = Carboxymethylcellulose

CNS = Central nervous systems

CZS = Congenital Zika Syndrome

CO₂ = Carbon dioxide

DAMPs = Damage-associated molecular pattern

DAPI = 4',6-diamidino-2-phenylindole

DENV = Dengue virus

DMEM = Dulbecco's Modified Eagle's Medium

DMEM/F12 = DMEM/F-12 = Dulbecco's Modified Eagle Medium (D-MEM/F12)

DNA = Deoxyribonucleic acid

FBS = Fetal bovine serum

G = Gravity

Gas6 = Growth arrest-specific 6 protein

GBS = Guillain-Barré syndrome

HBSS = Hank's Balanced Salt Solution

HIV = Human Immunodeficiency virus

HPI = Hour's post infection

HPV = Human papillomavirus

IBA-1 = Ionized calcium binding adaptor molecule 1

IIF = Indirect Immunofluorescence

INF-I = Type I interferon

INF- α = Alpha interferon

INF- β = Beta interferon

JEV = Japanese encephalitis virus

MDA5 = Melanoma differentiation-associated protein 5

MOI = Multiplicity of infection

mtDNA = Mitochondrial DNA

NPCs = Neural progenitor cells

ORF = Open Reading Frame
 PBS = Phosphate-buffered saline
 PFU = Plaque-forming unit
 NHP = Non-Human Primates
 PRRs = Pattern recognition receptor
 RIG-I = Retinoic acid-inducible gene I
 RNA = Ribonucleic acid
 RNAm = Messenger RNA
 RT-qPCR = Reverse transcription-quantitative polymerase chain reaction
 SARS-CoV = Severe acute respiratory syndrome associated coronavirus
 STAT2 = Signal transducer and activator of transcription 2
 STING or TMEM 173 = Stimulator of interferon genes or transmembrane protein 173
 TLR = Toll-like receptor
 WNV = West Nile virus
 YFV = Yellow Fever virus
 ZIKV = Zika virus

How to cite

SOUZA MPM, FREITAS BCG, HOLANDA GM, DINIZ JUNIOR JAP & CRUZ ACR. 2022. Correlation of *cGAS*, *STING*, *INF- α* and *INF- β* gene expression with Zika virus kinetics in primary culture of microglia and neurons from BALB/c mice. *An Acad Bras Cienc* 94: e20211189. DOI 10.1590/0001-3765202220211189.

Manuscript received on September 14, 2021; accepted for publication on February 14, 2022

MAYQUE PAULO M. DE SOUZA¹

<https://orcid.org/0000-0002-9298-6465>

BÁRBARA CAROLINE G. FREITAS¹

<https://orcid.org/0000-0001-9996-9388>

GUSTAVO M. HOLANDA¹

<https://orcid.org/0000-0001-6730-9254>

JOSÉ ANTÔNIO P. DINIZ JUNIOR²

<https://orcid.org/0000-0001-9432-138X>

ANA CECÍLIA R. CRUZ¹

<https://orcid.org/0000-0002-4607-9346>

¹Instituto Evandro Chagas (IEC/SVS/MS), Departamento de Arbovirologia e Febre Hemorrágica, Laboratório de Biologia Molecular, Rodovia BR-316, Km 7 s/n, Levilândia, 67030-000 Ananindeua, PA, Brazil

²Instituto Evandro Chagas (IEC/SVS/MS), Laboratório de Microscopia eletrônica, Seção de Hepatologia, Av. Alm. Barroso, 492, São Brás, 66093-020 Belém, PA, Brazil

Correspondence to: **Ana Cecília Ribeiro Cruz**

E-mail: anacecilia@iec.gov.br

Author contributions

MPMS and ACRC conceived the study and wrote the manuscript. MPMS processed the samples. MPMS and BCGF conducted the experiments. MPMS and GMH conducted the statistical analysis. ACRC, GMH and JAPDJ reviewed the paper. All authors read and approved the final manuscript.

